Supporting information for

Unusual stoichiometry, band structure and band filling in conducting enantiopure radical cation salts of TM-BEDT-TTF showing helical packing of the donors

Flavia Pop,[a] Cécile Mézière,[a] Magali Allain,[a] Pascale Auban-Senzier,[b] Naoya Tajima,[c] Daichi Hirobe,[d,e,f] Hiroshi M. Yamamoto, [d,e] Enric Canadell*[g] and Narcis Avarvari*[a]

[a] *Univ Angers, CNRS, MOLTECH-Anjou, SFR MATRIX, F-49000 Angers, France. E-mail:* narcis.avarvari@univ-angers.fr

[b] *Laboratoire de Physique des Solides, Université Paris-Saclay CNRS UMR 8502, Bât. 510, 91405 Orsay, France*

[c] *Department of Physics, Toho University, Funabashi, Chiba 274-8510, Japan*

[d] *Institute for Molecular Science, Myodaiji, Okazaki 444-8585, Japan*

[e] *SOKENDAI (Graduate University for Advanced Studies), Myodaiji, Okazaki 444-8585, Japan*

[f] *PRESTO, Japan Science and Technology Agency (JST), Kawaguchi 332-0012, Japan*

[g] *Institut de Ciència de Materials de Barcelona, ICMAB-CSIC, Campus de la UAB, E-08193 Bellaterra, Spain. E-mail:* canadell@icmab.es

X-Ray structure determinations

Single crystals of the compounds were mounted on plastic loops using a viscous hydrocarbon oil to coat the crystal and then transferred directly to cold nitrogen stream for data collection. X-ray data collection were performed at 150 K on a Rigaku Oxford Diffraction SuperNova with micro-focus CuKα (λ = 1.54184 Å) or on a Nonius Kappa CCD diffractometer, using graphite-monochromated MoK_α radiation (λ = 0.71073 Å). The structures solved by direct methods and refined on F^2 by full matrix least-squares techniques using SHELX programs [1] using the WinGX graphical user interface.[2] All non-H atoms were refined anisotropically and absorption was corrected using CrysAlisPro program (CrysAlisPro, Rigaku Oxford Diffraction, 2015 or 2019) or SADABS program (Sheldrick, Bruker, 2008). Hydrogen atoms were introduced at calculated positions (riding model), included in structure factor calculations but not refined. The four structure refinements containing solvent molecules showed disordered electron density which could not be reliably modeled and the program PLATON/SQUEEZE (A.L. Spek V290617 (1980-2019)) was used to remove the corresponding scattering contribution from the intensity data. This electron density can be attributed to chloroform or bromoform molecules. The assumed solvent compositions were used in the calculation of the empirical formula, formula weight, density, linear absorption coefficient, and F(000). A summary of the crystallographic data and the structure refinement is given in Table S1.

Table S1 Crystal Data and Structure Refinement at 150 K for $[(S)\text{-}\mathbf{1}]_9(Mo_6O_{19})_5$ and $[(R)\text{-}\mathbf{1}]_9(Mo_6O_{19})_5$ with both $CHCl_3$ and $CHBr_3$ together with the $[(rac)\text{-}\mathbf{1}]_2(Mo_6O_{19})$

Compound	$[(S)\text{-}\mathbf{1}]_9(Mo_6O_{19})_5$, 8.67 $CHCl_3$	$[(R)\text{-}\mathbf{1}]_9(Mo_6O_{19})_5$, 10 $CHCl_3$	$[(S)\text{-}\mathbf{1}]_9(Mo_6O_{19})_5$, 8.67 $CHBr_3$	$[(R)\text{-}\mathbf{1}]_9(Mo_6O_{19})_5$, 8.67 $CHBr_3$	$[(rac)\text{-}\mathbf{1}]_2(Mo_6O_{19})$
Empirical formula	$C_{134.67}H_{152.67}Cl_{26}Mo_{30}O_{95}S_{72}$	$C_{136}H_{154}Cl_{30}Mo_{30}O_{95}S_{72}$	$C_{134.67}H_{152.67}Br_{26}Mo_{30}O_{95}S_{72}$	$C_{134.67}H_{152.67}Br_{26}Mo_{30}O_{95}S_{72}$	$C_{28}H_{32}Mo_6O_{19}S_{16}$
Fw	9399.45	9558.60	10555.41	10555.41	1761.13
***T* (K)**	150.0(1)	150.0(1)	150.0(1)	150.0(1)	149.4(3)
Wavelength (Å)	0.71073	1.54184	1.54184	1.54184	1.54184
Cryst syst	Trigonal	Trigonal	Trigonal	Trigonal	Monoclinic
Space group	*R*32	*R*32	*R*32	*R*32	$P2_1/n$
***a* (Å)**	19.942(6)	19.7480(5)	19.7245(5)	19.6963(4)	12.2033(2)
***b* (Å)**	19.942(3)	19.7480(5)	19.7245(5)	19.6963(4)	15.5932(2)
***c* (Å)**	62.82(2)	62.405(3)	62.728(2)	62.6651(13)	13.9105(2)
α(deg)	90	90	90	90	90
***β*(deg)**	90	90	90	90	111.257(2)
***γ*(deg)**	120	120	120	120	90
***V* (Å^3)**	21635(15)	21076.3(14)	21135.2(13)	21053.6(10)	2466.91(7)
Z	3	3	3	3	2
D_c (g cm^{-3})	2.164	2.259	2.488	2.498	2.371
Abs coeff (mm^{-1})	2.089	18.849	20.493	20.572	19.087

---

[1] G. M. Sheldrick, (2013-2018) SHELXS-2013, SHELXL-2016 or 2018. Program for Crystal Structure solution and Crystal Structure refinement. University of Gottingen, Germany.

[2] L. Farrugia, *J. Appl. Crystallogr.*, 1999, **32**, 837–838.

Cryst size (mm^3)	0.26 x 0.22 x 0.04	0.114 x 0.083 x 0.014	0.386 x 0.223 x 0.052	0.292 x 0.101 x 0.036	0.385 x 0.068 x 0.041
Data collected / unique [Rint]	100276 / 8466 [0.138]	17736 / 8932 [0.046]	33677 / 9243 [0.080]	34906 / 9168 [0.080]	10926 / 5070 [0.051]
Data observed	4247	7176	8845	9013	4895
Flack parameter	0.09(16)	0.21(4)	0.19(4)	0.18(4)	-
GOF on F^2	1.019	1.042	1.058	1.056	1.164
Final R indices $[I > 2\sigma(I)]$[a]	0.0690/0.1582	0.0684/0.1846	0.0857/0.2377	0.0765/0.1726	0.0439/0.1177
R indices (all data)[a]	0.1611/0.2217	0.0806/0.1983	0.0875/0.2403	0.0777/0.1734	0.0475/0.1193
CCDC	2068677	2068680	2068681	2068682	2068683

[a] $R(F_o) = \Sigma||F_o| - |F_c||/\Sigma|F_o|$; $R_w(F_o^2) = [\Sigma[w(F_o^2 - F_c^2)^2]/\Sigma[w(F_o^2)^2]]^{1/2}$

$[\mathbf{1}]_9(\mathrm{Mo_6O_{19}})_5\cdot(\mathrm{CHCl_3})_x$ (x = 8.67 or 10)

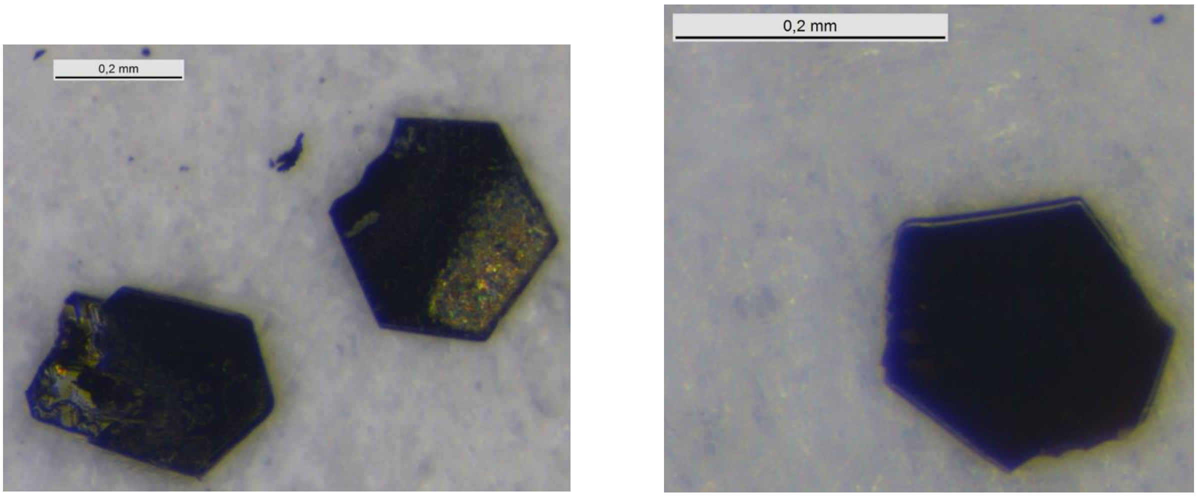

Fig. S1 Photos of crystals of $[(S)\text{-}\mathbf{1}]_9(\mathrm{Mo_6O_{19}})_5\cdot(\mathrm{CHCl_3})_2$.

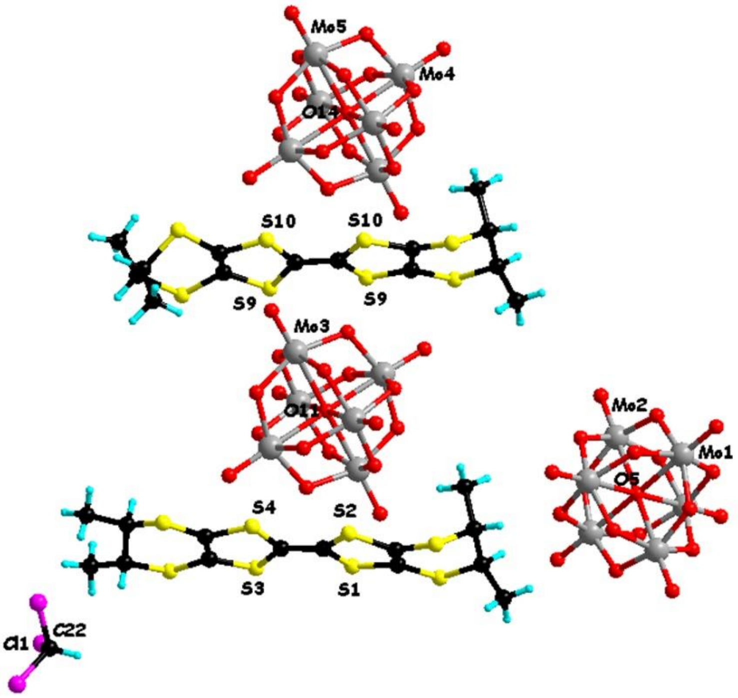

Fig. S2 Detail of the crystal structure of $[(R)\text{-}\mathbf{1}]_9(\mathrm{Mo_6O_{19}})_5\cdot(\mathrm{CHCl_3})_2$ with the two different donors (one and half independent), three different polyoxometallate dianions (two one third and one sixth independent) and a $\mathrm{CHCl_3}$ solvent molecule (one third independent).

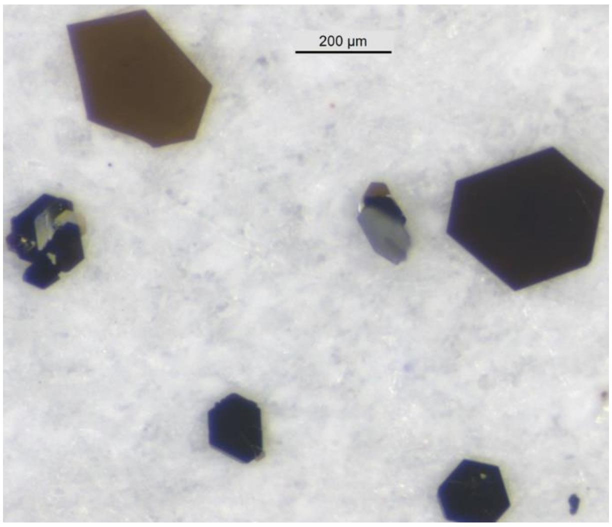

Fig. S3 Photos of crystals of $[(S)\text{-}\mathbf{1}]_9(Mo_6O_{19})_5{\cdot}(CHBr_3)_2$.

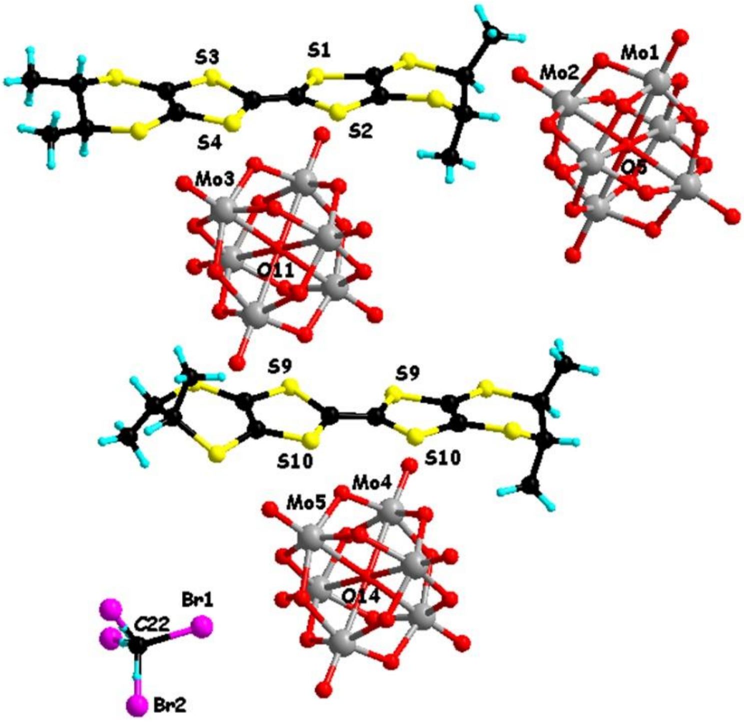

Fig. S4 Detail of the crystal structure of $[(S)\text{-}\mathbf{1}]_9(Mo_6O_{19})_5{\cdot}(CHBr_3)_2$ with the two different donors (one and half independent), three different polyoxometallate dianions (two one third and one sixth independent) and a $CHBr_3$ solvent molecule (one third independent).

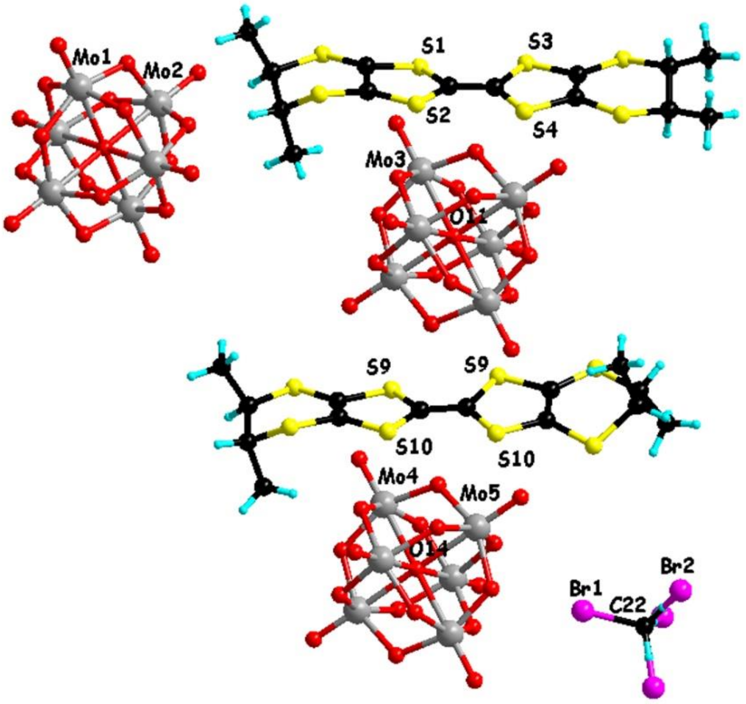

Fig. S5 Detail of the crystal structure of $[(R)\text{-}\mathbf{1}]_9(Mo_6O_{19})_5{\cdot}(CHBr_3)_2$ with the two different donors (one and half independent), three different polyoxometallate dianions (two one third and one sixth independent) and a $CHBr_3$ solvent molecule (one third independent).

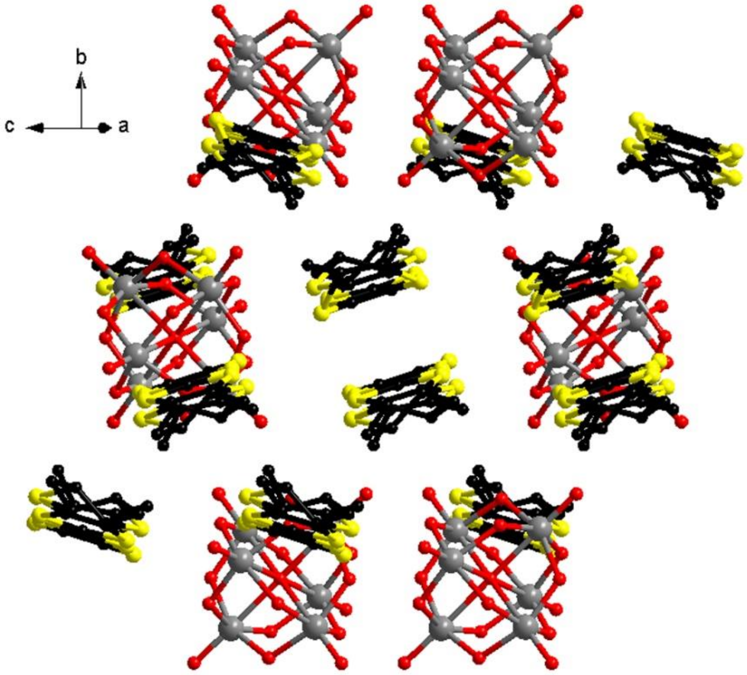

Fig. S6 Crystal packing in the structure of $[(rac)\text{-}\mathbf{1}]_2(Mo_6O_{19})$. Hydrogen atoms have been omitted.

Conductivity measurements

Electrical conductivity of [(*S*)-**1**]$_9$(Mo$_6$O$_{19}$)$_5$·(CHCl$_3$)$_2$ was measured on platelet-shaped single crystals 0.3-0.5 mm long. Gold wires were glued with silver paste on four aligned gold contacts previously evaporated on one face of the single crystals. Resistivity measurements were performed using an AC current of 1 µA and low-frequency (< 100 Hz) with lock-in amplifier detection. High hydrostatic pressures are applied in a homemade NiCrAl clamp type cell up to 2.3 GPa. The pressure is measured at room temperature when the pressure is varied using a manganin gauge and silicon oil (Idemitsu Daphne-oil 7373) is used as the pressure transmitting medium. Low temperature was achieved with a cryostat equipped with a 4 K pulse-tube.

The measurements of electrical conductivity on [(*R*)-**1**]$_9$(Mo$_6$O$_{19}$)$_5$·(CHBr$_3$)$_2$ were done by using conventional DC method with six-probes. Gold wires with the diameter of 15 µm were attached on the sample using carbon paste. Two electrodes were used for the current supply and other four electrodes for voltage sensors. A sample to which six electrical leads were attached was encased in a Teflon capsule filled with pressure medium (Idemitsu DN-oil 7373). The capsule was set in a clamp-type pressure cell made of MP35N hard alloy and hydrostatic pressure of up to 1.5 GPa was applied.

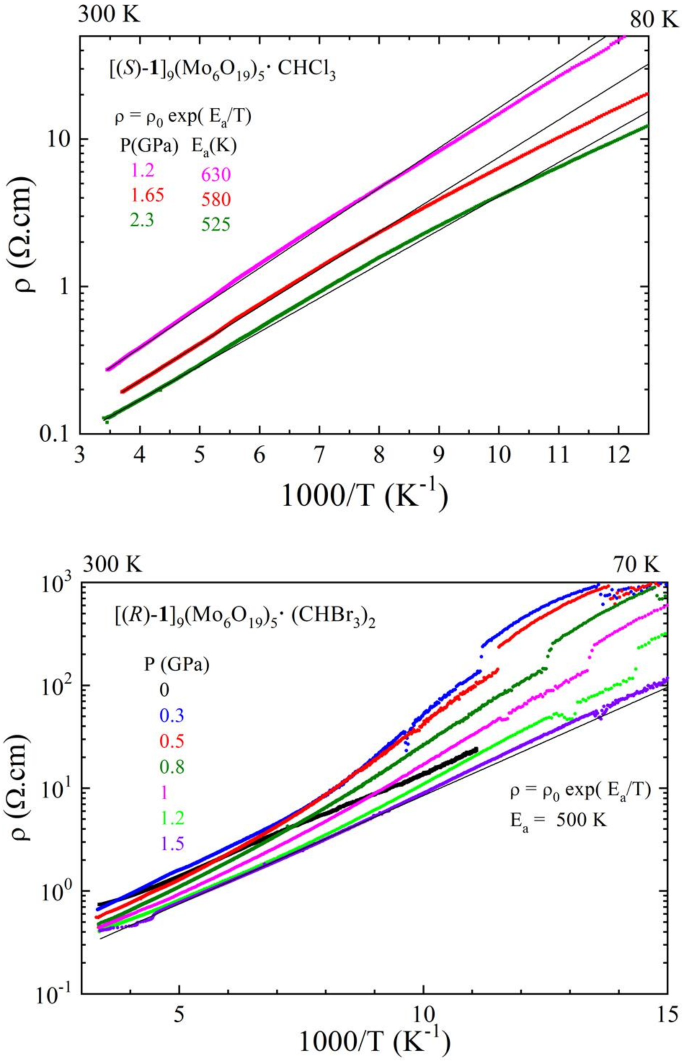

Fig. S7 Temperature dependence of the resistivity at different applied pressures for a single crystal of [(*S*)-**1**]$_9$(Mo$_6$O$_{19}$)$_5$·(CHCl$_3$)$_2$ (top) and for a single crystal of [(*R*)-**1**]$_9$(Mo$_6$O$_{19}$)$_5$·(CHBr$_3$)$_2$ (bottom) plotted as log ρ versus 1/T. The black lines are linear fit to the data giving the activation energy E$_a$.

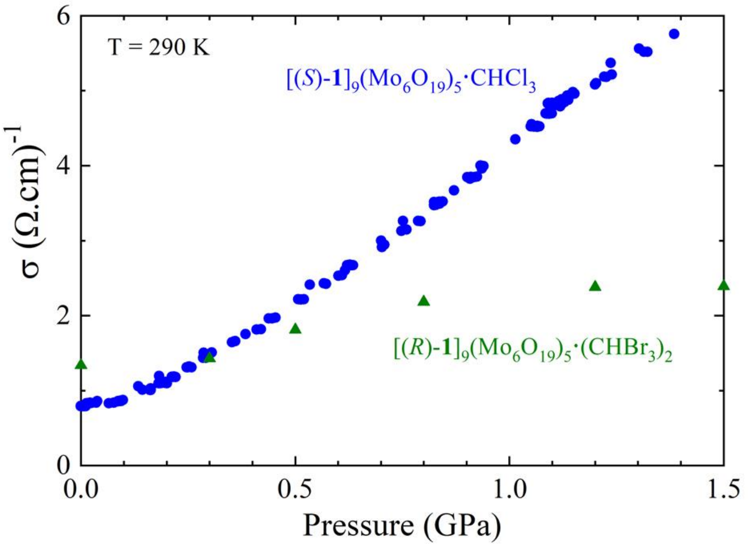

Fig. S8 Pressure dependence of the conductivity at room temperature for $[(S)\text{-}\mathbf{1}]_9(Mo_6O_{19})_5\cdot(CHCl_3)_2$ (blue circles) and for $[(R)\text{-}\mathbf{1}]_9(Mo_6O_{19})_5\cdot(CHBr_3)_2$ (green triangles).

Band structure calculations

The tight-binding band structure calculations were of the extended Hückel type.[1] A modified Wolfsberg-Helmholtz formula was used to calculate the non-diagonal $H_{\mu\nu}$ values.[2] All valence electrons were taken into account in the calculations and the basis set consisted of Slater-type orbitals of double-ζ quality for C 2s and 2p, S 3s and 3p and of single-ζ quality for H. The ionization potentials, contraction coefficients and exponents were taken from previous work.[3]

Table S2 S···S distances shorter than 3.9 Å and absolute values of the $\beta_{HOMO\text{-}HOMO}$ interaction energies (eV) for the different donor···donor interactions in the donor layers of [(*R*)-**1**]$_9$(Mo$_6$O$_{19}$)$_5$·(CHCl$_3$)$_2$

Interaction (type)	S···S (<3.9 Å)	$\lvert\beta_{HOMO\text{-}HOMO}\rvert$ (eV)
I (A-A)	3.445 (×2), 3.519 (×2), 3.565, 3.622 (×2),	0.1462
II (A-B)	3.620, 3.638, 3.707, 3.788, 3.823, 3.867	0.0962
III (A-B)	3.513, 3.525, 3.560, 3.678, 3.584, 3.685, 3.722	0.2299
IV (A-A)	3.443, 3.445 (×2), 3.514 (×2), 3.751 (×2)	0.2755

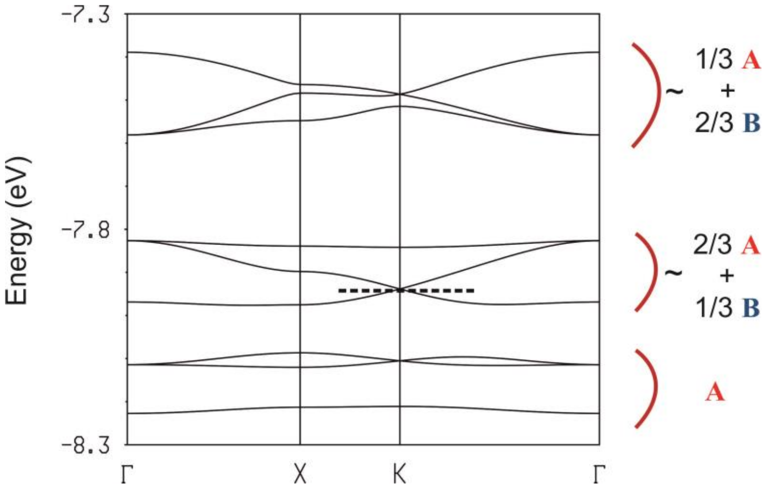

Fig. S9 Calculated band structure for the donor layers of [(*R*)-**1**]$_9$(Mo$_6$O$_{19}$)$_5$·(CHCl$_3$)$_2$ where Γ = (0, 0), X = (a*/2, 0) and K = (a*/3, a*/3). The dashed line indicates the highest occupied level assuming double occupation of the levels. The approximate composition of the bands is shown at the right hand of the diagram.

Table S3 S···S distances shorter than 3.9 Å and absolute values of the $\beta_{HOMO-HOMO}$ interaction energies (eV) for the different donor···donor interactions in the donor layers of [(*R*)-**1**]$_9$(Mo$_6$O$_{19}$)$_5$·(CHBr$_3$)$_2$

Interaction (type)	**S···S (<3.9 Å)**	**|$\beta_{HOMO-HOMO}$| (eV)**
I (A-A)	3.439 (×2), 3.498 (×2), 3.510, 3.625 (×2),	0.1372
II (A-B)	3.581, 3.625, 3.689, 3.785, 3.787, 3.849	0.0890
III (A-B)	3.434, 3.491, 3.501, 3.535, 3.575, 3.674, 3.723	0.2465
IV (A-A)	3.439, 3.468 (×2), 3.5142(×2), 3.762 (×2)	0.2810

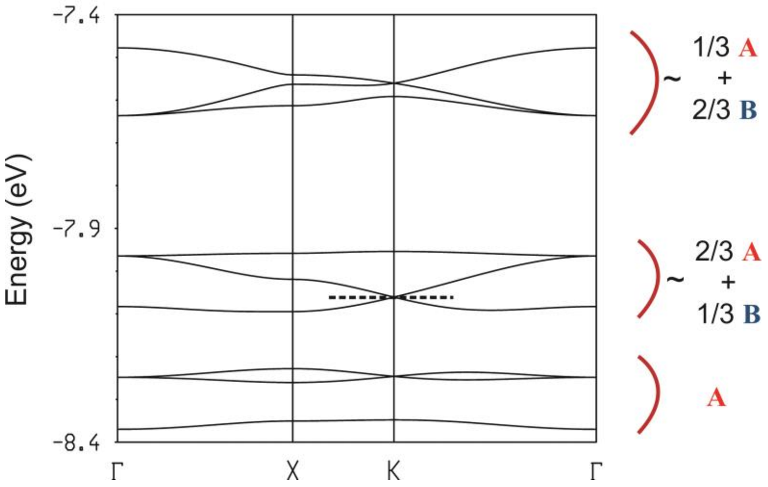

Fig. S10 Calculated band structure for the donor layers of [(*R*)-**1**]$_9$(Mo$_6$O$_{19}$)$_5$·(CHBr$_3$)$_2$ where Γ = (0, 0), X = (a^*/2, 0) and K = (a^*/3, a^*/3). The dashed line indicates the highest occupied level assuming double occupation of the levels. The approximate composition of the bands is shown at the right hand of the diagram.

References

1 M.-H. Whangbo and R. Hoffmann, *J. Am. Chem. Soc.*, 1978, **100**, 6093-6098.

2 J. H. Ammeter, H.-B. Bürgi, J. Thibeault and R. Hoffmann, *J. Am. Chem. Soc.*, 1978, **100**, 3686-3692.

3 A. Pénicaud, K. Boubekeur, P. Batail, E. Canadell, P. Auban-Senzier, D. Jérome, *J. Am. Chem. Soc.*, 1993, **115**, 4101-4112.

FET measurements

Thin single crystal of $[(S)\text{-}\mathbf{1}]_9(Mo_6O_{19})_5\cdot(CHBr_3)_2$ was grown in a round flask equipped with two platinum electrodes, where electrochemical oxidation was performed for three hours in the same condition described in the main text. During the oxidation process, the current was gradually increased from 3 μA to 5 μA. Thin crystal with a thickness less than 300 nm was transferred by pipette from the flask to a petri dish filled with small amount of isopropanol and was laminated onto a SiO_2(300 nm)/p++Si substrate with pre-patterned gold electrodes (Au 18 nm/Ti 2nm). The Si substrate was used as a bottom gate electrode that can accumulate electrostatically doped excess carriers at the interface layer of $[(S)\text{-}\mathbf{1}]_9(Mo_6O_{19})_5\cdot(CHBr_3)_2$. The gate voltage dependence of the device resistance was measured by standard d.c. four probe method to exclude the effect of contact resistance.